

# IN-FLIGHT MEASUREMENT OF WING SURFACE PRESSURE DISTRIBUTION ON A FIXED-WING UAV AND ITS APPLICATION TO FLIGHT CONTROL

Yusuke Hayashi<sup>1</sup>, Ju-Hoe Kim<sup>1</sup> & Takeshi Tsuchiya<sup>1</sup>

<sup>1</sup>The University of Tokyo, Japan

#### **Abstract**

Birds utilize their feathers, enveloping both wings and bodies, to perceive airspeed and detect airflow separation. Additionally, birds dynamically adjust the geometry of their wings to adapt to varying flight conditions. In contrast, conventional tube-and-wing aircraft rely on gyroscopes and accelerometers for attitude estimation but often lack sensors to measure airflow around their wings. Inspired by the birds' airflow sensors, several simple methods of sensing airflow around the wing were devised in previous research. The methods involved embedding multiple pressure sensors in the wing surface. In this study, a pressure distribution measurement system using several small absolute pressure sensors was developed. Research utilizing the measured pressure values for flight control is planned. A rigid fixed-wing UAV is planned to be used to test the flight control systems.

Keywords: Pressure Sensor Array, Fixed-Wing UAV, Flight Control, Bird

#### 1. Introduction

With the advent of commercial use of UAVs and urban air mobility, in addition to conventional aircraft, the use of airspace is expected to increase dramatically. The increase of aircraft in the air may lead to increase an in carbon dioxide emission and accidents and deterioration in convenience due to congestion. Although research is being conducted to address these issues, such as hydrogen fuel and electrification, most remain in the form of conventional tube-and-wing aircraft. This research aims to break away from the conventional form of fixed-wing aircraft and achieve even higher efficiency, safety, and convenience by imitating birds. To accomplish higher efficiency, angle of attack (AoA) will be precisely controlled to maximize L/D. To increase safety and convenience, signs of flow separation will be detected to avoid stall and increase agility by utilizing high AoA. Achievement will be demonstrated by flight tests of an experimental UAV.

Birds can detect airspeed and separation of flow around the wings by the feathers covering their wings and bodies [1], and achieve high flight performance by altering the wing geometry [2]. On the other hand, fixed-wing aircraft, excluding experimental ones, are rarely equipped with sensors that sense flow around the wings. The use of a pressure sensor array as a substitute for bird feathers to function as an airflow sensor was investigated in past research.

Enumerating related studies, Brown and Fedde investigated the feasibility of measuring AoA and airspeed using a one-dimensional array of thin capacitive pressure sensors with a thickness of less than 1 mm attached to the main wing of a UAV through simulation[3]. Bunge, Alkurdi and Alfaris measured pressure during stall and spin using multiple pressure sensors embedded in the wing of a UAV[4]. Mohamed, Watkins and Fisher measured the wing surface pressure distribution of a UAV in a wind tunnel generating turbulence and the position of pressure measurement ports suitable for flight control based on pressure data was verified[5]. Araujo-Estrada, Salama and Greatwood incorporated strain gauges and pressure sensors into a wing and compared strain and pressure values in a wind tunnel with turbulence with those from actual flight. Furthermore, roll control using strain data in the

#### IN-FLIGHT PRESSURE DISTRIBUTION MEASUREMENT FOR UAV FLIGHT CONTROL

wind tunnel and pitch control using estimated AoA from pressure sensor data were implemented[6]. Borup, Fossen and Johansen placed pressure sensors on the wing, nose, and side of the fuselage and estimated AoA and sideslip using neural networks and regression analysis[7]. Heinrich developed a method to estimate AoA and stall using a differential pressure sensors inside a wing and used the method to control a fixed-wing UAV in a deep stall landing[8].

# 2. Pressure Sensor Array Design

# 2.1 Sensor Type Selection

In previous research, several types of pressure sensors were used to measure the pressure distribution around the wing. The types are differential pressure sensors with two or more ports and absolute pressure sensors. In addition to these sensors, a film-type pressure sensor was added to the consideration list. Table 1 summarizes the advantages and disadvantages of using each sensor. Considering that the sensors will be installed in a small UAV, absolute pressure sensor was selected for this research because of its advantages in terms of weight and size.

Sensor Type	Pros	Cons	
Differential Pressure Sensor (Single Port)	Accuracy o	Price, Weight △,Size×	
Differential Pressure Sensor (Multi-Port)	Accuracy ∘	Price, Tubing, Weight, Size ×	
Absolute Pressure Sensor	Price, Weight, Size o	Accuracy △	
Film-type Sensor	Installation o Surface smoothness o	Accuracy, Range, Weight ×	

Table 1 – Pros and cons of using differential, absolute, and film pressure sensors.

#### 2.2 Electronics

The sensor array is implemented by connecting multiple sensor modules with 8 sensors on board in a daisy chain connection. A microcontroller reads the sensor data via one or more SPI buses. The chip select signals for SPI bus are generated by a shifting register on each sensor module to reduce signal lines. By doing so, the daisy chained sensor module can be controlled and read by only 7 wires while maintaining a clock speed higher than  $1MH_Z$ .

## 2.3 Sensor Arrangement

As for sensor arrangement, two methods were considered. The first method was placing the sensors on a printed circuit board (PCB) parallel to the ribs with tubes extending to the wing surface. The second was placing the sensors parallel to the wing skin by using a flexible PCB. In terms of the flexibility of pressure measurement location, sensor protection, cost, wiring weight, and ease of maintenance, the first method was selected. The tubing required in the first method was printed by a fused deposition modeling (FDM) 3D printer.

## 2.4 3D Printed Tubes

As mentioned above, the tubing were manufactured by a FDM 3D printer with the configuration shown in Table 2. The configuration was determined with a view to reducing leakage by strengthening the bond between layers. The channels have a minimum width of 0.5mm and are separated from each other as much as possible to prevent leak. The interface between the tubing and the printed circuit board mounted with absolute pressure sensors are filled with sealing material to prevent leak. Figure 1 shows the CAD view of the 3D print tube.

## 3. Wind Tunnel Test of Prototype Pressure Sensor Array

The prototype sensor module with 8 Bosch Sensortec BMP388 absolute pressure sensors on board is shown in Figure 2. The system is designed to form an 2 dimensional sensor array by connecting multiple modules shown in the upper part of Figure 2.

#### IN-FLIGHT PRESSURE DISTRIBUTION MEASUREMENT FOR UAV FLIGHT CONTROL

Parameter	Value	Reason
Material	PLA	Dimensional stability and availability.
Layer Height	$0.05mm \sim 0.10mm$	Prevent leak by improving interlayer bond.
Hot End Temperature	$205^{\circ}C \sim 220^{\circ}C$	"
Filament Flow Rate	105%	"

Table 2 – 3D printer configuration for printing tubes.

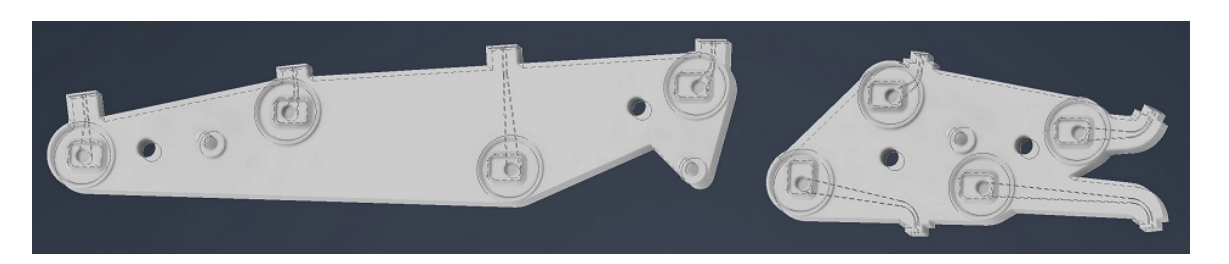


Figure 1 – CAD view of the prototype 3D printed tube.

A wind tunnel experiment was conducted to test whether the selected sensor has enough resolution and noise level to measure the pressure distribution around a wing and to check the characteristics of the airfoil.

The prototype sensor module to be tested has 6 ports that measure wing top surface pressure at 6%, 20%, 32.5%, 45%, 57.5%, 70%c and 2 ports for the bottom at 6%, 20%c. The module was installed into a 3D printed wing section as shown in figure 3.The wing has 1000mm span, 250mm chord length, no taper and no twist.

# 3.1 Experiment Setup

The assembled wing section was mounted on a 6-axis force sensor in a low speed Gottingen wind tunnel with an open test section as shown in figure 4. Although, the output of the fan of the wind tunnel can be controlled discretely, the flow velocity was set to around 10m/s. As the flow velocity changes for each condition due to drag, readings of a manometer was recorded and was used to calculate  $C_L$ ,  $C_D$  and  $C_P$ . The AoA was changed every  $2^\circ$  from  $-10^\circ$  to  $+20^\circ$  degrees. The AoA of the wing was measured by an inertial measurement unit mounted inside the wing assuming that the flow is parallel to the ground. One sensor measuring the pressure of the top surface had an initial failure and could not measure the pressure at 32.5%c. The pressure sensors were setup to measure pressure at  $25H_Z$  the built in low-pass filter was enabled.

## 3.2 Results

The aerodynamic coefficients that were calculated from the 6-axis force sensor measurements are shown in Figure 5. Absolute pressure data histories for each AoA are shown in Figure 6. Regrettably, the atmospheric pressure was not logged during the experiment. Atmospheric pressure history data from an weather station approximately 2.7km from the wind tunnel facility was used to compensate the atmospheric pressure change in the calculation of  $C_P$ .  $C_P$  calculated by averaging the absolute pressure sensor measurements and  $C_P$  values estimated by VSPAERO are shown in Figure 7.

Figure 6 shows that the sensor noise levels are smaller than the pressure difference between other ports. In addition, as the wing section approaches stall angles, increase in amplitude of pressure at the suction side was observed. Once the wing section stalled, pressure close to the leading edge on the suction side suddenly increased.

Figure 7 shows that, although trends in measured and VSPAERO estimated  $C_P$  values are generally consistent, a port close to the leading edge on the bottom side showed  $C_P \le 1$ . It may be due to the difference of the reference atmospheric pressure and the atmospheric pressure at sensor calibration as the atmospheric pressure increased about 20Pa in 10 minutes before the experiment, which is equivalent to about 0.3 in  $C_P$ . It is hard to say because the calibration time was not recorded, but there may be an overall offset of about 0.3.

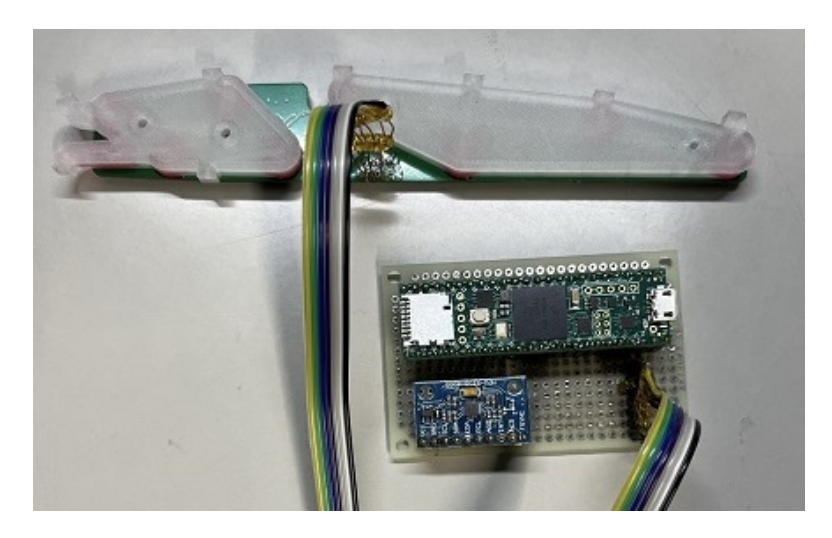


Figure 2 – Prototype sensor module and logging board.

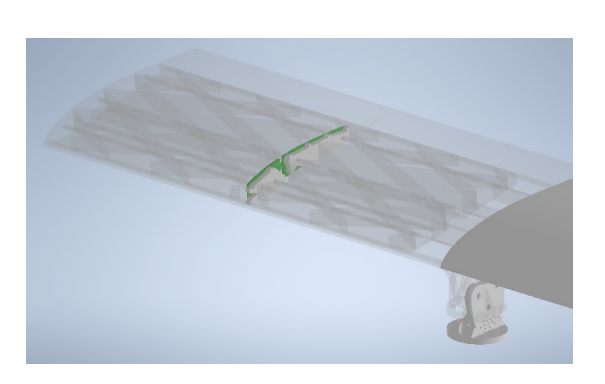
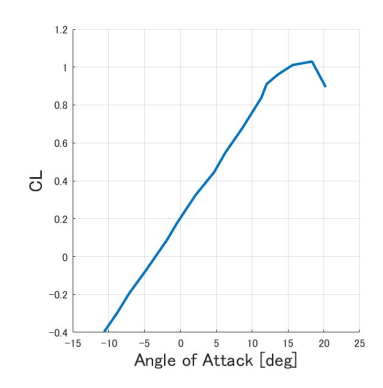
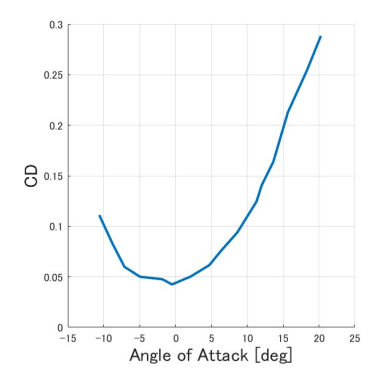


Figure 3 – CAD image of prototype sensor module in 3D printed wing section.



Figure 4 – Wing section with sensor module set up in a wind tunnel.





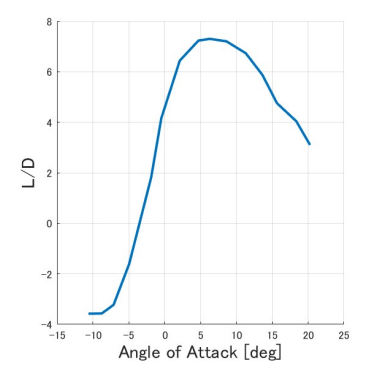


Figure  $5 - C_L, C_D, L/D$  by AoA

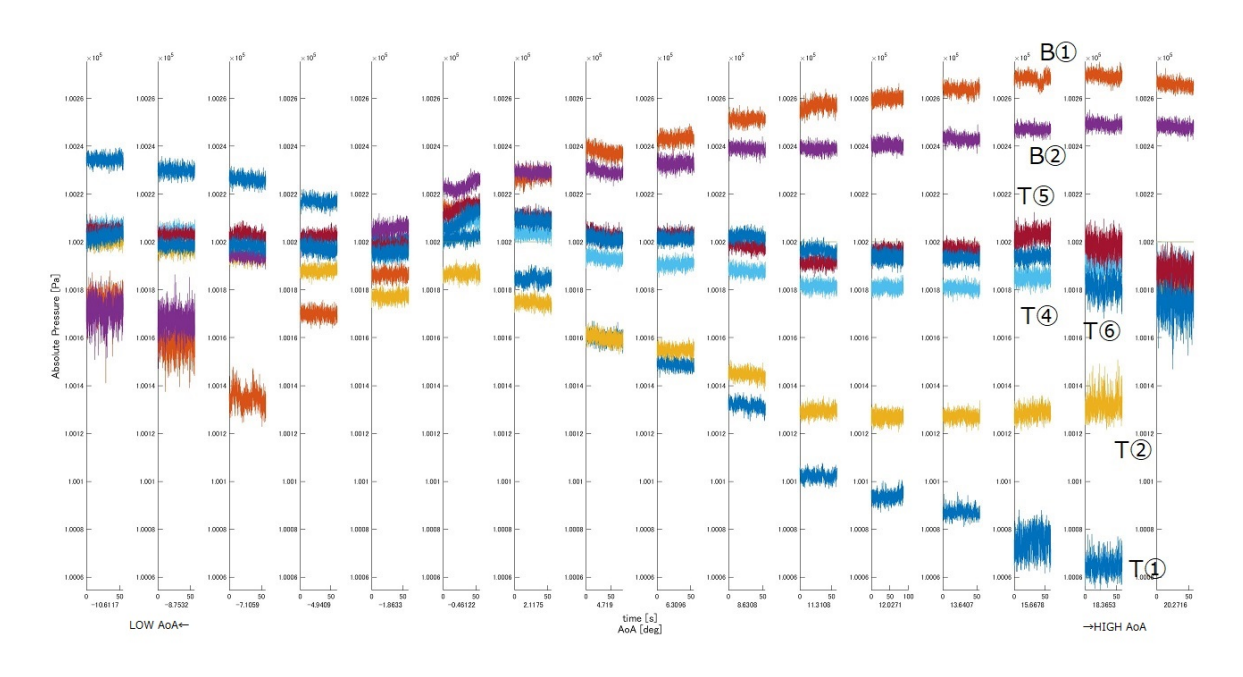


Figure 6 – Absolute pressure history for each AoA.  $T^{\textcircled{1}} \sim T^{\textcircled{6}}$  represent ports on the top side of the wing at 6%, 20%, 45%, 57.5%, 70%c and  $B^{\textcircled{1}}, B^{\textcircled{2}}$  represent ports on the bottom side of the wing at 6%, 20%c. Sensor for port at 32.5%c faced an error so  $T^{\textcircled{3}}$  is skipped.

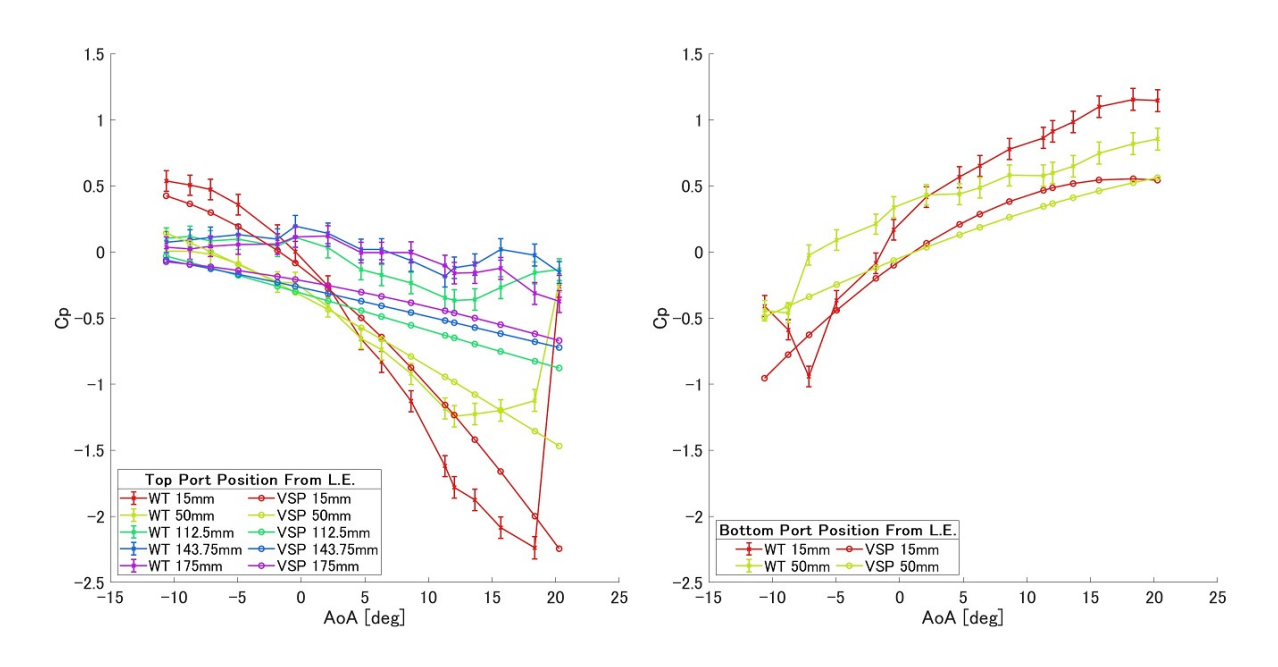


Figure 7 –  $C_P$  plotted against AoA. WT is for the values obtained from the wind tunnel experiment, and VSP is for the values estimated using VSPAERO. The error bars indicate the uncertainty of  $C_P$  due to the 10Pa resolution of the atmospheric pressure data provided by Japan Meteorological Agency.

# 4. Flight Testing of the Pressure Sensor Array System

The pressure sensor array was mounted on a fixed-wing UAV testbed and in-flight measurement tests were conducted.

# 4.1 Fixed-Wing UAV Testbed

To test the pressure sensor array, a small fixed-wing UAV was used. Table 3 shows the specifications and Figure 8 is the picture of the UAV used. The main wing was newly built so that it would fit

Parameter	Value	Parameter	Value
Span	1.750 <i>m</i>	Length	1.180m
Main Wing Area	$0.392m^2$	Weight	2kg
Propulsion	Electric Motor + Propeller		

Table 3 – Fixed wing UAV specifications.



Figure 8 – Fixed-wing UAV that was used for the flight test.

4 pressure sensor modules on each side. The wings are mainly made out of balsa wood, and are designed so that the pressure sensor modules can be easily replaced. Since the wings are covered with film, holes were cut out for the pressure measuring ports. Figure 9 shows how the sensor module is mounted inside the wing.

# 4.2 System Configuration

## 4.2.1 Pressure Sensor Array

Based on the wind tunnel test, a new version of the pressure sensor array with some small modifications was developed. The new version uses STMicroelectronics LPS22HHTR absolute pressure sensors where Bosch Sensortec BMP388s were used in the prototype. To fit the printed circuit boards in the tapered main wing, the PCB was designed much smaller than the prototype and the sensors were arranged in a regular pattern. Pressure sensors were assembled on a daughter board in a group of 4 and 2 of them were mounted on a carrier board so that sensors can be easily replaced in case of a malfunction. 3D printed tubes were custom made for each wing section to handle the different chord length. The ports were placed at 6%, 20%, 33%, 45%, 57.5%, 70%c for the top side and 6%, 20%c for the bottom side. Figure 10 shows the ports on the top side of the wing. The ports have  $2.5mm \times 4mm$  openings at the surface of the wing and the covering film is cut out at the ports.

Although 4 sensor modules can fit in each side of the wing, 3 modules were implemented in each wing. The modules were placed at 319.5mm, 454.5mm, 589.5mm to the span direction from the center of the wing. A total of 6 modules were implemented in the wings and as each module has 8 sensors, 48 sensors measured the wing surface absolute pressure in the flight test. 2 SPI buses were used to control and read the sensors. The sensors measured pressure at 200Hz and did not use the optional filtering function of the sensor.

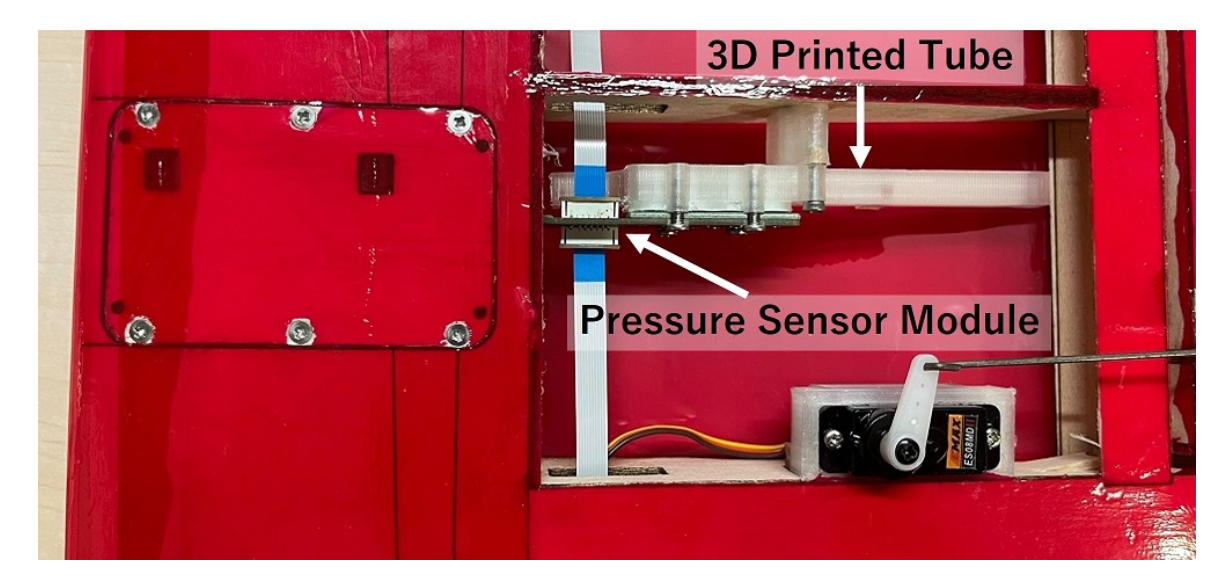


Figure 9 – Bottom view of the main wing with a pressure sensor module forming the pressure sensor array system.

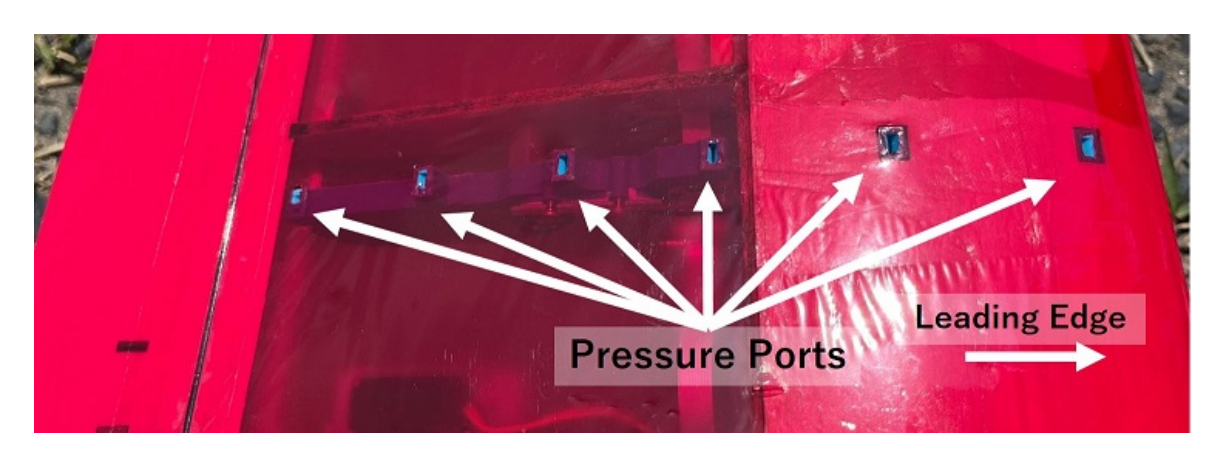


Figure 10 – Top view of the main wing. 6 pressure ports are visible in the picture.

## 4.2.2 Flight Controller

In this particular flight test, no novel flight control methods were introduced. However, to obtain flight data such as attitude and to gain further stability of the aircraft, Pixracer running PX4 was mounted inside the fuselage. A microcontroller gathering pressure data from the pressure sensor array works with Pixracer, logging pressure sensor array data and major flight data at the same time. Flight system diagrams are shown in Figure 11. Actuator Command Signal seen in this diagram was not used for this flight test.

## 4.3 Results

3 flights were done in 2 days. In the first test, the pressure sensor array could not measure pressure properly due to the small holes that were made on the covering film and insufficient sealing material which could not lead pressure to the sensor elements. After solving this problem by enlarging the holes and adding extra sealant, the second and third flights were conducted. Before the second flight, thermal deformation was observed in the 3D printed tubes as seen in the aftmost port in Figure 10 due to the heat generated by prolonged exposure to sunlight. However, more than half the area of the ports were exposed, so the experiment was continued. In the second flight, 1 pressure sensor did not function properly.

In the third flight, every sensor worked fine. With the help of the stabilization function of PX4, the aircraft performed several hard rolling, pitching and yawing maneuvers. In addition to this, the aircraft was intentionally stalled several times. The pressure sensor array data for the entire flight is shown in Figure 12, detailed data for a hard pitching maneuver is shown in Figure 13 and a stall in 14. There

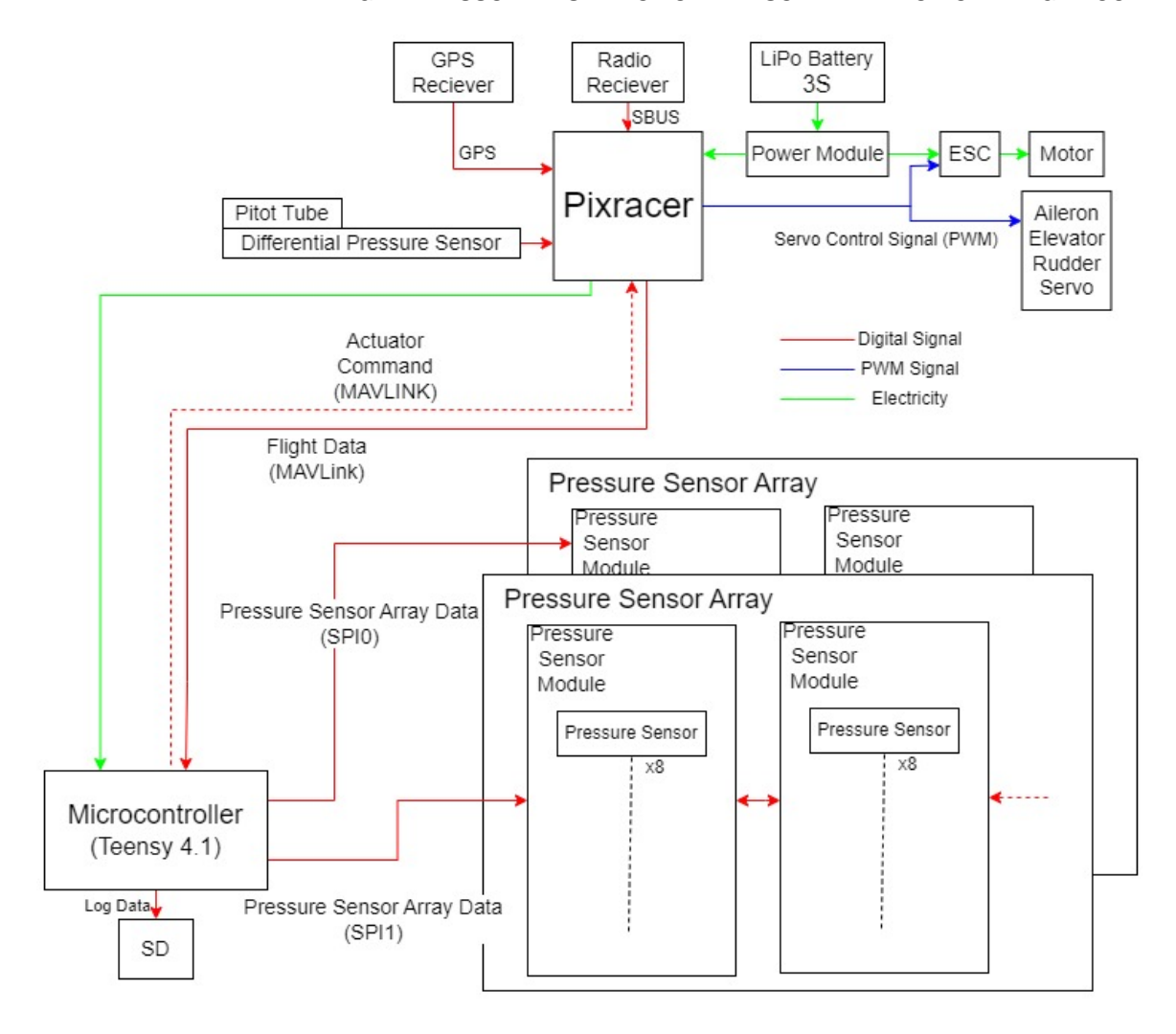


Figure 11 – Flight systems onboard the UAV.

were some missing values due to SD card write error, so they were supplemented by the previous value of the same sensor.

## 4.4 Discussion

Although the sensor offset was eliminated by post-processing averaging the first 2000 samples, pressure sensor array data showed a maximum pressure difference of 20Pa soon after landing when there is minimal airspeed. It may be due to the temperature change of the sensors as the sunlight heated sensors cooled down by the wind in flight. Since sensor drift is practically unavoidable, the effect must be evaluated and taken into account in the development of a flight control method.

Differences in amplitude were observed between each sensor module. As seen in Figure 12 and 13, sensor modules on the left wing constantly indicated smaller pressure differences than modules on the right.

In the pitching maneuver, shown in Figure 13, although the peak time of acceleration to the Z-axis, where high AoA is expected, matched with the peak pressure and showed similar trend to the numerical results at high AoA, meaning the developed sensor array system somehow measured pressure distribution around the wing, as mentioned above, differences in amplitude were observed between each sensor module.

In Figure 14, when the UAV was intentionally stalled, sudden increase of pressure were observed by the sensors measuring the top side of the wing close to the leading edge (ports T1,T2) while B1 and B2 remained still starting at around t = 496s. According to the previous wind tunnel test, oscillation of pressure is expected, but in flight, changes in angle of attack occur so rapidly that, practically speaking, there is no time to detect oscillations. It is necessary to establish a mechanism for detecting

signs of stalling that does not rely on oscillation detection.

Further analysis on the aforementioned issues using wind tunnels and flight tests is required.

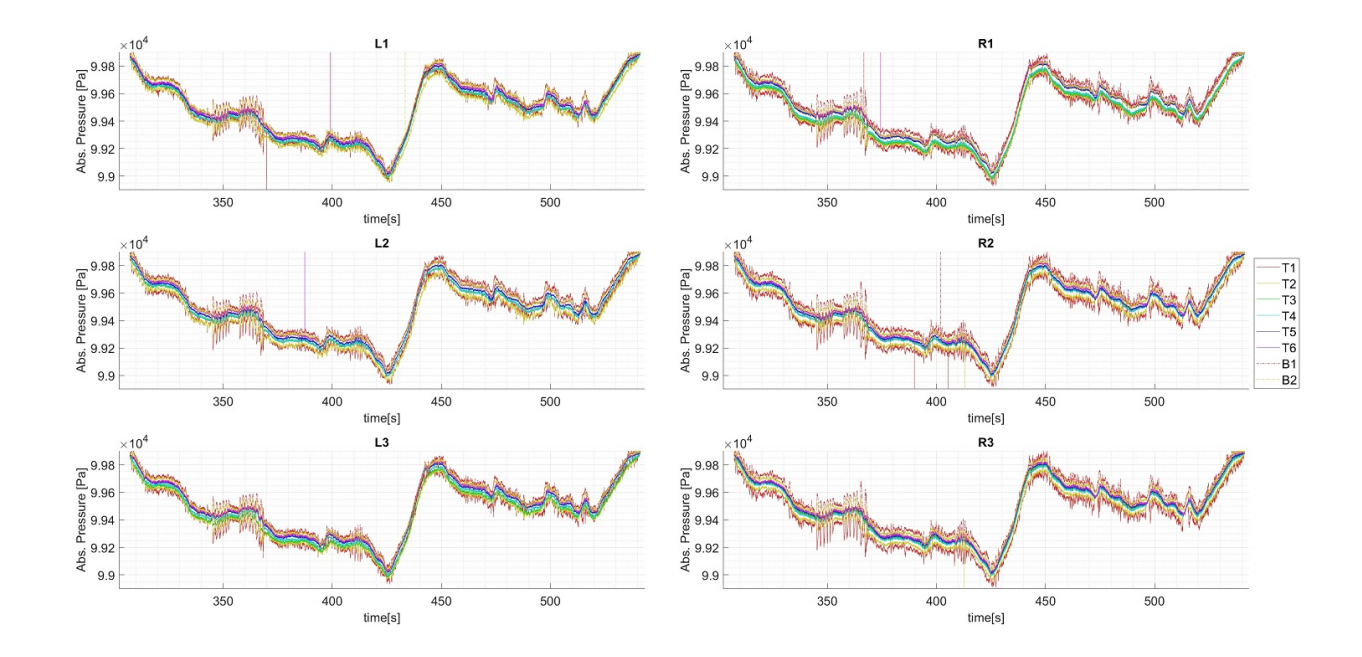


Figure 12 – In-flight pressure sensor array data throughout the flight. Pressure measurements for each module are shown. Modules are numbered from the inner wing side. T1 $\sim$ 6 indicate pressure on the top side of the wing at 6%, 20%, 33%, 45%, 57.5%, 70%c. B1 $\sim$ 2 indicate pressure on the bottom side of the wing at 6%, 20%c.

## 5. Flight Control Plans

AoA estimating and stall detecting methods involving machine learning proposed in [7] [8] will be implemented in the flight system developed in this research and will be tested. Implementation of another method to estimate the AoA from pressure measurements by referring to the results of numerical simulations of the wing is planned. A flight control method utilizing the estimated AoA and signs of stall will be developed whose main function is to control the AoA with precision and to prevent the aircraft from entering the stall region. These functions will be tested in flight.

## 6. Conclusion

A wing surface pressure measuring sensor array system was developed. It was tested in a wind tunnel and in flight. The developed pressure sensor array system was found to be capable of measuring the wing surface pressure distribution but has some issues to be solved which are sensor drift problems and difference of amplitude between sensor modules. As soon as these issues are resolved a flight control method utilizing the pressure data will be developed and tested in flight.

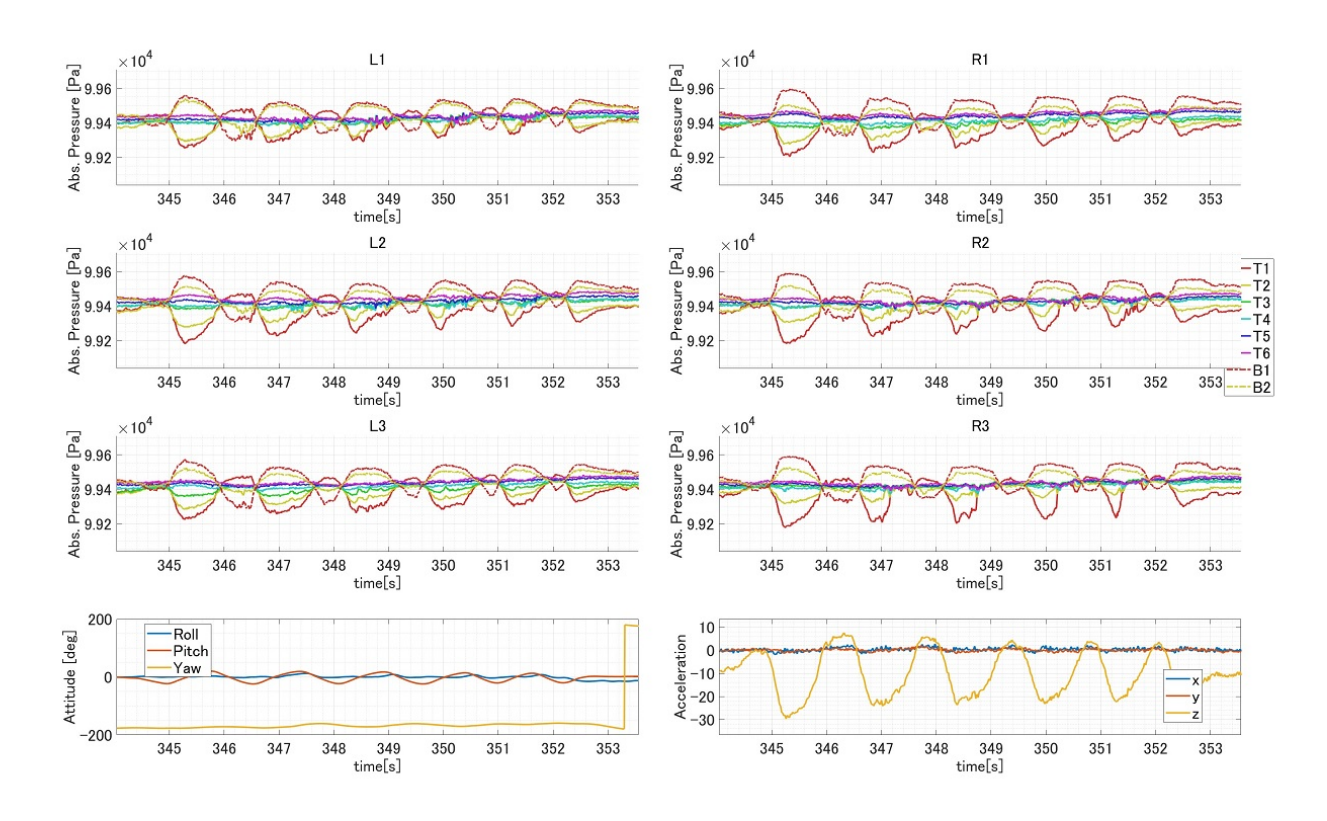


Figure 13 – Pressure sensor array, attitude and acceleration data in several hard pitch up and down maneuvers.

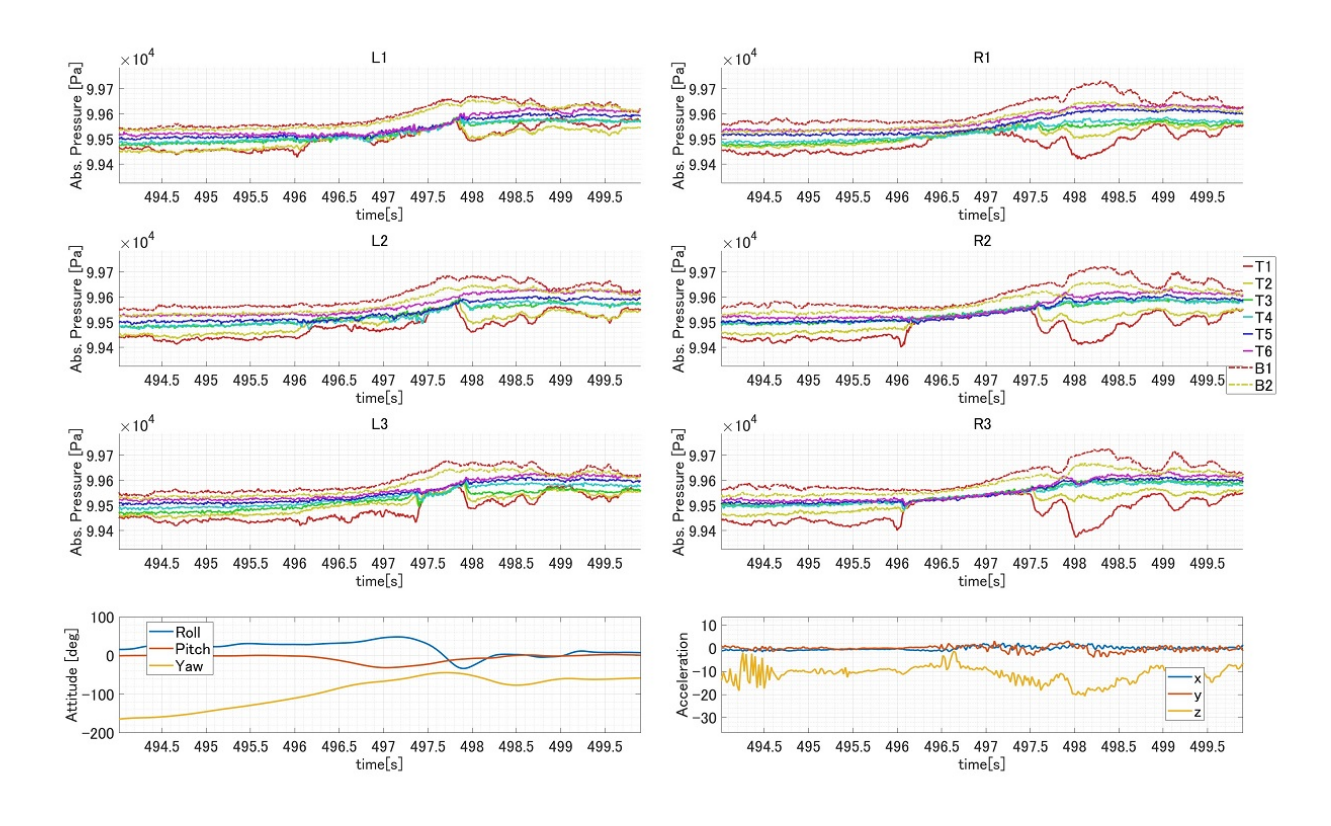


Figure 14 – Pressure sensor array, attitude and acceleration data in an intentional stall.

# 7. Acknowledgement

This work was supported by JSPS KAKENHI Grant Number JP23K17333.

## 8. Contact

Yusuke Hayashi:

E-mail Address: yhayashi747@g.ecc.u-tokyo.ac.jp

Mailing Address:

The University of Tokyo,

Faculty of Engineering, Bldg. No.7 Department of Aeronautics and Astronautics,

Tsuchiya Lab

7-3-1 Hongo Bunkyo-ku 113-8656 Tokyo Japan

# 9. Copyright Statement

The authors confirm that they, and/or their company or organization, hold copyright on all of the original material included in this paper. The authors also confirm that they have obtained permission, from the copyright holder of any third party material included in this paper, to publish it as part of their paper. The authors confirm that they give permission, or have obtained permission from the copyright holder of this paper, for the publication and distribution of this paper as part of the ICAS proceedings or as individual off-prints from the proceedings.

#### References

- [1] BROWN, R.E., and FEDDE, M.R., "AIRFLOW SENSORS IN THE AVIAN WING," Journal of Experimental Biology, Vol. 179, No. 1, 1993, pp. 13-30.
- [2] Lentink, D., de Kat, R., Henningsson, P., "How swifts control their glide performance with morphing wings," Nature, Vol. 446, No. 7139, 2007, pp. 1082-1085.
- [3] Callegari, S., Talamelli, A., Zagnoni, M., "Aircraft angle of attack and air speed detection by redundant strip pressure sensors," IEEE, Piscataway NJ, 2004, pp. 1526-1529 vol.3.
- [4] Roberto A. Bunge, Abdul E. Alkurdi, Eyas Alfaris, "In-Flight Measurement of Wing Surface Pressures on a Small-Scale UAV During Stall/Spin Maneuvers," AIAA Flight Testing Conference, American Institute of Aeronautics and Astronautics, 2016,
- [5] Mohamed, A., Watkins, S., Fisher, A., "Bioinspired Wing-Surface Pressure Sensing for Attitude Control of Micro Air Vehicles," Journal of Aircraft, Vol. 52, No. 3, 2015, pp. 827-838.
- [6] Araujo-Estrada, S.A., Salama, F., Greatwood, C., "Bio-inspired Distributed Strain and Airflow Sensing for Small Unmanned Air Vehicle Flight Control," AIAA Guidance, Navigation, and Control Conference, American Institute of Aeronautics and Astronautics, 2017,
- [7] Borup, K.T., Fossen, T.I., and Johansen, T.A., "A Machine Learning Approach for Estimating Air Data Parameters of Small Fixed-Wing UAVs Using Distributed Pressure Sensors," IEEE Transactions on Aerospace and Electronic Systems, Vol. 56, No. 3, 2020, pp. 2157-2173
- [8] Heinrich, Gian-Andrea, "Learning to Stall, Using in-air pressure data to identify, characterise and control fixed-wing aircraft stall", ETH Zurich, 2020